Molecular Neurobiology
https://doi.org/10.1007/s12035-024-04392-1

RESEARCH

Differential Alterations in the Expression of AMPA Receptor and Its Trafficking Proteins in the Hippocampus Are Associated with Recognition Memory Impairment in the Rotenone-Parkinson's Disease Mouse Model: Neuroprotective Role of *Bacopa monnieri* Extract CDRI 08

Vartika Gupta[1] · **S. Prasad**[1]

Received: 17 December 2023 / Accepted: 21 July 2024

Abstract
Parkinson's disease (PD), an age-associated neurodegenerative motor disorder, is associated with dementia and cognitive decline. However, the precise molecular insight into PD-induced cognitive decline is not fully understood. Here, we have investigated the possible alterations in the expression of glutamate receptor and its trafficking/scaffolding/regulatory proteins underlying the memory formation and neuroprotective effects of a specialized *Bacopa monnieri* extract, CDRI-08 (BME) in the hippocampus of the rotenone-induced PD mouse model. Our Western blotting and qRT-PCR data reveal that the PD-induced recognition memory decline is associated with significant upregulation of the AMPA receptor subunit GluR1 and downregulation of GluR2 subunit genes in the hippocampus of rotenone-affected mice as compared to the vehicle control. Further, expressions of the trafficking proteins are significantly upregulated in the hippocampus of rotenone-affected mice compared to the vehicle control. Our results also reveal that the above alterations in the hippocampus are associated with similar expression patterns of total CREB, pCREB, and BDNF. BME (CDRI-08, 200 mg/kg BW) reverses the expression of AMPA receptor subunits, their trafficking proteins differentially, and the transcriptional modulatory proteins depending on whether the BME treatment was given before or after the rotenone treatment. Our data suggest that expression of the above genes is significantly reversed in the BME pre-treated mice subjected to rotenone treatment towards their levels in the control mice compared to its treatment after rotenone administration. Our results provide the possible molecular basis underlying the rotenone-induced recognition memory decline, conditions mimicking the PD symptoms in mouse model and neuroprotective action of bacoside A and bacoside B (58%)–enriched *Bacopa monnieri* extract (BME) in the hippocampus.

Keywords Parkinson's disease · Recognition memory · Cognition · AMPA receptor · GluR1 · GluR2 · *Bacopa monnieri* · BME (CDRI-08) · AMPAR trafficking proteins

Introduction

Parkinson's disease (PD) is a prevalent neurological disorder that affects around 1% of the global population aged 65 years or/and above [1]. The aetiology of the disease is attributed to the degeneration of dopaminergic neurons in the substantia nigra pars compacta region of the brain due to aggregation of Lewy bodies composed of mis-folded α-Synuclein protein. PD is primarily characterized by bradykinesia, resting tremors, postural instability, and rigidity [2–4]. As the disease advances, individuals with PD also experience non-motor symptoms, such as impairments in executive function, memory consolidation, recalling, and processing information which leads to cognitive deficits [5–7]. Reports suggest that PD leads to dementia, referred as PD-induced dementia (PDD) [8, 9]. However, the precise mechanism underlying PD-induced cognitive impairment is not fully understood. Cognition is strongly associated with neuronal plasticity which is hampered in neurodegenerative conditions [10].

✉ S. Prasad
s.sprasadbhu@gmail.com

[1] Biochemistry and Molecular Biology Laboratory, Department of Zoology, Institute of Science, Banaras Hindu University, Varanasi 221005, UP, India

Published online: 29 July 2024

Several studies are going on to explore the mechanism by which the synaptic plasticity is achieved involving the long-term potentiation (LTP) and long-term depression (LTD) as they play crucial role in memory formation [11]. The establishment of LTP, an important pathway for the development of learning and memory, occurs in the hippocampus and is governed by two major ionotropic glutamate receptors: α-amino-3 hydroxyl-5 methyl-4-isoxazole-propionate receptor (AMPAR) and N-methyl-D-aspartate receptor (NMDAR) [12–16]. In order to stabilize and regulate these receptors on the postsynaptic membrane, proteins such as PICK-1 (Protein Interacting with C Kinase 1), PSD-95 (Postsynaptic Density Protein 95), and TARP γ-2 (Transmembrane AMPA Receptor Regulatory Protein Gamma-2) play crucial role. PICK-1 is involved in the trafficking and targeting of AMPA receptors by interacting with the GluR2 subunit of AMPA receptors and regulates their internalization. PICK-1 is also involved in the control of other receptors and channels [17]. One of the main scaffolding proteins in excitatory synapses' postsynaptic density is PSD-95, a protein that belongs to the family of proteins called membrane-associated guanylate kinases (MAGUKs). It is essential for the synapse's organization and securing of signalling chemicals. In order to help synaptic proteins at the postsynaptic membrane, PSD-95 interacts with a variety of synaptic proteins, such as AMPA and NMDA receptors. This clustering is essential for synaptic plasticity and memory formation, as well as for the effective transfer of information between neurons [18]. A member of the TARPs, which are AMPA receptor auxiliary subunits, is TARP γ-2. TARPs alter AMPA receptor trafficking, gating characteristics, and synaptic location. Particularly connected to AMPA receptors in the brain, TARP γ-2 is essential for synaptic activity [17]. To control synaptic strength and plasticity, which aids in learning and memory processes, TARPs and AMPA receptors must interact [19]. Altogether, these proteins have a role in the assembly of signalling complexes at excitatory synapses as well as the control of glutamate receptors, especially AMPA receptors. The establishment of memory and synaptic plasticity depends on the dynamic control of these proteins.

The LTP pathway is initiated by the release of glutamate from pre-synaptic neurons which activates the AMPA receptor at postsynaptic density and depolarization of the postsynaptic membrane. Depolarization of the postsynaptic membrane activates NMDAR by removing the Mg^{2+} block to achieve postsynaptic potential (PSP) which in turn allows extracellular Ca^{2+} and Na^{+} influx in the neurons [20–23]. The Ca^{2+} binds to the CaMKIIα that mediates the expression of more AMPAR and NMDAR on the postsynaptic membrane as well as activates transcription factor cAMP–response element binding protein (CREB) [24] for regulating gene expression of various synaptic plasticity–related proteins such as brain-derived neurotrophic factor (BDNF) [16, 23]. BDNF plays an important role in hippocampal memory formation by regulating several neuronal activities and neuron survival. These factors have the potential to serve as a focus for understanding PD-associated cognitive impairment and also aid to the potential therapeutic treatment of memory decline due to PD. One of the neuromodulatory herbs *Bacopa monnieri* is used in the present study to see its neuroprotective as well as neurotherapeutic role in PD and PD-induced cognitive impairment.

Bacopa monnieri, also referred to as Brahmi, is a well-known herbal plant that has been utilized in the traditional Indian medicinal system (Ayurveda) for centuries. Its extract has been employed as a nerve tonic to address a wide range of neurological disorders associated with memory [24–26]. *Bacopa monnieri* extract (BME) contains saponins such as bacosides, flavonoids, bacosaponines, and bacopaside N1 [27, 28]. BME has an anti-inflammatory, anti-apoptotic, antioxidative, and memory-boosting role in many neurological diseases [29–31]. Numerous scientific investigations indicate that *B. monnieri* alcoholic extract and saponins, in particular bacoside A and bacoside B, may boost cognitive functions by improving memory and learning [32]. BME (CDRI-08) has been found to improve memory impairment in amnesic and diabetes conditions [33, 34]. Regarding the cognitive enhancement attributed to *B. monnieri*, various mechanisms of action have been suggested. These include antioxidant neuroprotection, reduction of β-amyloid, inhibition of acetylcholinesterase (AChE), modulation of neurotransmitters such as dopamine (DA), 5-hydroxytryptamine (5-HT), and acetylcholine (ACh), as well as binding of muscarinic cholinergic receptors, activation of choline acetyltransferase, elevation of cerebral blood flow, modulation of hypothalamic-pituitary-adrenal (HPA) axis output, and protection of the hippocampus [29, 32–38]. The hippocampus of the brain is primarily associated with memory formation. Hippocampus has three important regions: the dentate gyrus (DG) and the cornu ammonis region (CA3 and CA1). DG initiates the processing of information and CA3 and CA1 are involved in the acquisition and retrieval of memory [39].

In the light of its nootropic effect, the present study has been designed to study the effects of *Bacopa monnieri* extract (CDRI-08) on AMPA receptor subunits: GluR1 and GluR2, their trafficking proteins and regulatory molecules (total CREB, pCREB, and BDNF), and neurodegeneration in the hippocampus of rotenone-induced PD-mimicking mouse model.

Materials and Methods

Animals

Inbred male Swiss albino mice were maintained at an optimum temperature (25 ± 1 °C), photoperiods (12-h light/dark cycle) with unrestricted access to standard mice food

and water. The mice were cared under the guidelines set by the Committee for Control and Supervision of Experiments on Animals (CPCSEA). All experimental procedures were approved by the Institutional Animal Ethical Committee of Banaras Hindu University, Varanasi (Approval no.: BHU/DOZ/IAEC/2021–2022/007, Dated 15/02/2022).

Chemicals

All chemicals utilized in the research were of analytical and molecular grades, procured from reputable suppliers such as Sigma, Merck, SRL, and Qualigens India. The primary antibodies used in this study were α-Synuclein, GluR1, GluR2, PSD95, TARPγ-2, PICK-1, CREB, pCREB, BDNF, and cleaved Caspase-3. These antibodies were procured from DSHB, Peprotech, Imgenex, Bioss, and Neuromab-UCDavis, USA. The secondary antibody used was HRP-conjugated (Genie, Bangalore, India) and Fluorophores tagged (AbCam, USA). The standardized extract of *Bacopa monnieri* Extract (BME)-CDRI-08 was graciously provided by Dr. H. K. Singh (former Director, CDRI, Lucknow, India). CDRI-08 contains approximately 55 ± 5% of bacosides A and B.

Grouping, Drug Preparations and Administration

The mice were divided into four groups, each consisting of nine mice. The groups were as follows: (1) control group, which received dimethyl sulfoxide (DMSO) subcutaneously for 14 days, and after that 5% Tween 80 was given orally; (2) rotenone-treated group, which received 2 mg/kg BW rotenone dissolved in DMSO subcutaneously for 14 days; (3) rotenone pre-treated with *Bacopa monnieri* extract (BME) group, which received 200 mg/kg BW of BME dissolved in 5% Tween 80 orally for 21 days before administration of rotenone; and (4) rotenone post-treated with *Bacopa monnieri* extract (BME) group, which received 200 mg/kg BW of BME dissolved in 5% Tween 80 orally for 21 days after administration of rotenone. After the completion of treatments, behavioural evaluation was conducted and subsequently, the mice were sacrificed, followed by decapitation. The hippocampus was then isolated for RNA isolation and protein homogenate preparation for qPCR and Western blotting, respectively. The brain was stored at − 80 °C for the cryosections for IFC.

Grip-Strength Test

The grip-strength test was conducted using a Medicraft grip-strength meter to evaluate the maximal muscle strength of the forelimbs in mice. Each mouse was gently grasped by the tail and allowed to hold onto the horizontal bars that were linked to the sensor. The mouse was subjected to a retrograde force, and the maximum force exerted by the animal was measured in kilograms. Each mouse underwent the identical treatment three times [40].

Rotarod Test

The rotarod test involved placing mice on a rotating rod. The rotational speed of the standard testing apparatus was increased from 5 to 15 revolutions per minute (rpm) for 120 s per mouse for three consecutive days. On the fourth day, the time it took for each mouse to fall off the spinning rod (referred to as latency) was measured and recorded [41].

Elevated Plus Maze Test

The elevated plus maze (EPM) test is used to measure anxiety-like behaviour in rodents. The apparatus consists of four arms in plus-shaped orientation with each arm length of 36 cm and width of 6 cm in which two arms are enclosed by 15 cm high walls oriented opposite to each other forming closed arms. The two remaining arms are open arms. The plus maze was elevated above ground level by 60 cm. Mice were placed on the intersection of the plus maze and allowed to walk for 5 min which was recorded. ANY-maze software (version 7.2, Stoelting Co., USA) was used to analyze the videos. The time spent in the open arm and the number of entries in the open arm were plotted in the graph [42].

Novel Object Recognition Test

Novel object recognition (NOR) test is comprised of habituation, training, and test tasks. Mice were habituated in a 50 cm × 50 cm × 40 cm open field for 5 min without objects. After 24 h of habituation, training began. Two similar-shaped and sized objects were placed in an open field. The mice were then introduced one by one into the open field for 5 min and recorded while they explored the two objects. The training was done twice in 28 h. Test sessions were conducted 48 h after the last training session by replacing a familiar object with a novel one. Mice were then placed in the box and allowed to explore for 5 min, which was recorded. ANY-maze software (version 7.2, Stoelting Co., USA) was used to analyze the videos. Mouse interaction with objects is measured by mouse head entry in the periphery. Time spent with the novel object was calculated as TNovel / (TNovel + TFamiliar), time spent with the familiar object was calculated as TFamiliar / (TNovel + TFamiliar), and Discrimination Index (DI) for the novel object was calculated as (TNovel − TFamiliar) / (TNovel + TFamiliar) [43].

Western Blot Analysis

To analyze the expression of proteins, the pooled hippocampus tissue was mechanically homogenized in RIPA buffer containing 150 mM NaCl, 2 mM EDTA, 50 mM Tris–HCl (pH 7.4), 1% Triton X-100, 0.5% sodium deoxycholate, 0.1% SDS, PMSF, and protease inhibitor cocktail. The protein concentration of the sample was assessed by the Bradford reagent [44]. The proteins of different groups were separated by SDS-PAGE [45] and transferred onto a PVDF membrane by wet transfer method. The membrane was blocked in blocking solution (5% non-fat skimmed milk in TBST) for 3 h at room temperature; the membranes were then incubated overnight with their respective primary antibodies α-Synuclein (DSHB-S1-890 H3C-s-Supernatant), GluR1 (DSHB-S1-1880, N355/1-supernatant), GluR2(DSHB-S1-1881, L21/32-supernatant), anti-PICK-1 (UC-Davis-Neuromab, L20/8), anti-PSD-95(UC-Davis-Neuromab, K28/43), anti-CREB (IMGENEX, IMG-271), pCREB (Bioss, bs-0036R), BDNF (Peprotech, 500P-84), and cleaved Caspase-3 (Bioss, bsm-33199 M). Thereafter, membranes were washed in TBST and incubated in appropriate HRP-conjugated secondary antibodies at a dilution of 1:2000 (Genei Laboratories, India). The membrane was washed in TBST, and signals were detected using the ChemiDoc imager (AI680) by the ECL method. As an internal control for normalization, the same blot was stripped and probed with an anti-β-actin HRP-conjugated antibody (Sigma, A3854). Blots were scanned and quantified by AlphaEase FC (Alpha Imager 2200) software.

qRT-PCR (Quantitative Reverse Transcription PCR)

To check the expression of GluR1 (*GRIA-1*) and GluR2 (*GRIA-2*) at the transcript level, qRT-PCR was done. To carry out this, first RNA was isolated using TRI reagent (Sigma-Aldrich, USA) [46] and cDNA was synthesized taking 5 µg RNA. Amplification was done using cDNA as template DNA with specific primers and Power Up SYBR Green master mix (Thermo Fisher Scientific, USA) for GluR1 (F-5′GAACGAAGGACTGTCAACATG3′; R-5′AGAGCT TCCTGTAGTTCCG3′) and GluR2 (F-5′CAGTGCATTTCG GGTAGG3′; R-5′TTGGTGACTGCGAAACTG3′) β-actin (F-5′ATCGTGGGCCGCTCTAGGCACC3′; R-5′CTCTTT GATGTCACGCACGATTTC3′) as endogenous control was used for normalization. The relative fold change in gene expression was calculated using the $2-\Delta\Delta CT$ method [47].

Immunofluorescence Cytochemistry (IFC)

To check the expression of α-Synuclein, GluR1, and GluR2 in hippocampal subregions, IFC was performed according to Dalvi and Belsham [48]. Initially, the brain was transcardially perfused with 4% paraformaldehyde (PFA) to fix the brain, after completion of perfusion brain tissue was incubated in 4% PFA overnight. Then, the brain was cryopreserved with a different gradient of sucrose solution (10%, 20%, and 30%). Then, the tissue was embedded in OCT and coronal Sects. (10 µm thick) were obtained using a cryostat (Leica Biosystem, Germany). These sections were then affixed onto slides that had been coated with poly-L-lysine. The cryosections were incubated for 1 h at 37 °C until the water evaporated. To remove the cryomount, the dried sections were washed three times in 1XPBS buffer (2.7 mM KCl, 137 mM NaCl, 4.0 mM KH2PO4, 4.3 mM Na_2HPO_4, pH 7.4) for 5 min each. Sections were permeabilized for 40 min with 1% TritonX-100 in 1X PBS buffer, then washed with the same buffer to remove excess TritonX-100. Thereafter, sections were treated for 2 h with 5% normal goat serum (NGS) to suppress non-specific proteins. In a humidity chamber, sections were treated overnight with diluted α-Synuclein (DSHB-S1-890H3C-s-Supernatant), GluR1 (DSHB-S1-1880 N355/1-supernatant), and GluR2 (DSHB-S1-1881 L21/32-supernatant), primary antibody (0.5 µg/µl in 2% NGS-1X PBS solution). The next day, following three 1X PBS washing at room temperature, sections were then treated for 2 h at room temperature in the dark with FITC (for α-Synuclein) and TRITC (for GluR1 and GluR2)–labelled goat anti-mouse anti-IgG secondary antibodies at 1:250 dilution in 2% NGS-1X PBS buffer. The sections were then washed in 1X PBS buffer, treated with DAPI for 10 min at room temperature, and mounted with an antifade mounting solution containing DABCO and glycerol. By omitting the primary antibody, a negative control slide was also made to identify the non-specific signals. Photomicrographs were taken at 40 × magnification using a Laser scanning super-resolution microscope (Confocal microscope). The immunofluorescence signal for α-Synuclein, GluR1, and GluR2 expression was evaluated using ZEISS ZEN blue software area integrated density measuring tool.

Nissl's Staining

The hippocampus sections were submerged in 95% ethyl alcohol at room temperature for 5 h. They were then rinsed for 5 min in 75% ethyl alcohol and then for five more minutes in distilled water. The sections were incubated for 30 min in a solution containing 0.1% cresyl violet acetate (Nissl's stain) that had been heated to 60 °C. Thereafter, the sections were rinsed in distilled water. The specimens were submerged in 75% ethanol, 90% ethanol for 2 min, and 100% ethanol for 2 min for a brief period for dehydration. The sections were then mounted with DPX after undergoing a 2-min xylene-clearing procedure [29]. The slide was examined using a bright-field microscope (Leica, Germany).

Statistical Analysis

The data acquired from the behavioural analysis, qRT-PCR, Western blotting, and immunofluorescence chemistry (IFC) were statistically analyzed by one-way ANOVA followed by Tukey's post hoc test after performing the Shapiro-Wilk normality test. The values are represented as mean ± SEM. Statistical analysis was conducted with SPSS 16.0 for Windows, and $p < 0.05$ was considered statistically significant.

Results

Effect of BME on Altered Motor Behaviour in Rotenone-Affected Mice

The neuromuscular and skeletal strength of mice is evaluated using a method called the grip-strength test. As seen in Fig. 1A, the treatment of rotenone resulted in a significant ($p < 0.05$) reduction in the grip strength of rotenone-affected mice as compared to the group that served as the control. However, mice that were post-treated with BME had a significant ($p < 0.05$) rise, although to a lesser extent than mice that were pre-treated with BME. The effects of BME pre-treatment on mice had more potential to suppress these effects. Furthermore, rotarod test for locomotion and balance showed that rotenone-affected mice spent much less time ($p < 0.05$) on the revolving rod compared to the control group. When comparing mice that were pre-treated and post-treated with BME, it was observed that the mice spent a significantly longer time on the revolving rod, which suggests an improvement in their motor behaviour. Nevertheless, the mice that received pre-treatment of BME exhibited a more noticeable impact compared to the mice that received post-treatment of BME, when compared to the rotenone-affected mice (Fig. 1B).

Effect of BME on α-Synuclein Expression Alteration in Hippocampus Due to Rotenone Treatment

The level of α-Synuclein expression is significantly elevated ($p < 0.05$) in mice affected with rotenone in comparison to mice in the control group. Nevertheless, the rotenone-affected mice that received pre- and post-BME treatment exhibited a significant reduction in the expression of altered α-Synuclein compared to the normal control mice (Fig. 2A, B). Furthermore, immunofluorescence labelled immunohistochemistry (IHC) in the dentate gyrus (DG), cornu ammonis-3 (CA3), and cornu ammonis-1 (CA1) regions of the hippocampus in brain slices (Fig. 2C–H) showed a comparable pattern to that reported in the Western blot analysis data. In brief, the expression level of α-Synuclein was significantly elevated in the DG, CA3, and CA1 areas of the hippocampus in rotenone-affected mice when compared to control mice. The administration of BME before and after rotenone-affected mice resulted in significant amelioration of α-Synuclein levels. However, the immunohistochemistry (IHC) data indicated that the pre-treatment had a much greater amelioration capability compared to the post-BME treatment.

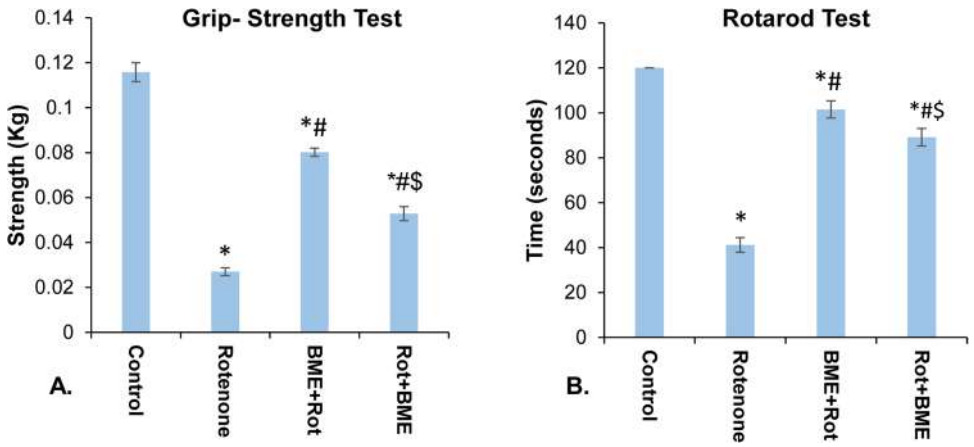

Fig. 1 Effects of BME (CDRI-08) on the motor coordination in vehicle-treated control, rotenone-affected mice (PD), pre-BME-treated PD mice (BME + Rot), and post-BME-treated PD mice (Rot + BME). Grip strength (kg) (**A**); latency time to fall (Sec) of mice on the Rotarod (**B**). Data present mean ± SEM; *, a significant difference ($p < 0.05$) between control and other groups; #, a significant difference ($p < 0.05$) between rotenone and BME groups; $, significant difference ($p < 0.05$) between BME + Rot and Rot + BME groups

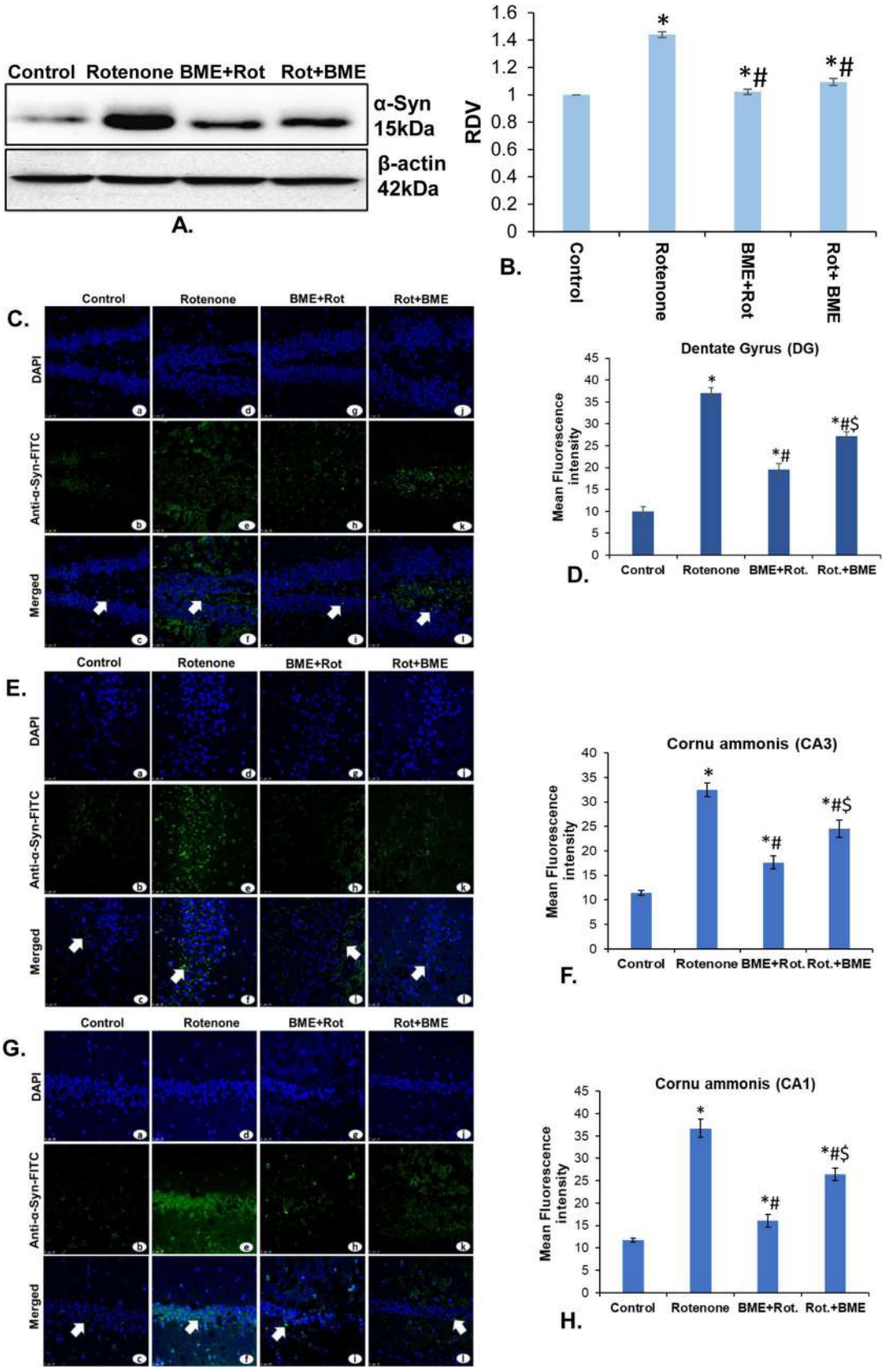
Control
Rotenone
BME+Rot
Rot+BME
α-Syn 15kDa
β-actin 42kDa
A.
RDV
B.
Dentate Gyrus (DG)
Mean Fluorescence intensity
D.
Cornu ammonis (CA3)
F.
Cornu ammonis (CA1)
H.
C.
E.
G.
DAPI
Anti-α-Syn-FITC
Merged

◂**Fig. 2** Effects of BME (CDRI-08) on the expression of the α-Synuclein protein in the hippocampus of vehicle-treated control, rotenone-affected mice (PD), pre-BME-treated PD mice (BME + Rot), and post-BME-treated PD mice (Rot + BME). Western blot analysis of α-Synuclein and β-actin (**A**). Histogram represents RDV of α-Synuclein (monomer) (IDV of α-Synuclein/IDV of β-actin) (**B**); photomicrographs show immunofluorescence illustrating FITC-labelled signals of α-Synuclein in DG (**C**), CA3 (**E**), and CA1 (**G**) region of the hippocampus; histogram represents mean fluorescence intensity of DG (**D**), CA3 (**F**), and CA1 (**H**) regions of hippocampus. Data represent mean ± SEM; *, a significant difference ($p < 0.05$) between control and other groups; #, a significant difference ($p < 0.05$) between rotenone and BME groups; $, significant difference ($p < 0.05$) between BME + Rot and Rot + BME groups

Effect of BME on Altered Recognition Memory in Rotenone-Affected Mice

The novel object recognition (NOR) test was conducted to observe the impact of BME on the modified recognition memory caused by PD. The rotenone-affected mice exhibited a significant decrease ($p < 0.05$) in the time spent exploring novel objects compared to the control mice. The exploration time of the novel object significantly increased ($p < 0.05$) in both pre- and post-treated mice compared to rotenone-affected mice, as a result of the pre- and post-treatment with BME. Furthermore, the discrimination index of rotenone-affected mice was considerably reduced ($p < 0.05$) compared to control mice. Both pre-treated and post-treated mice had significantly higher discrimination index (DI) compared to PD mice (Fig. 3A–C).

Effect of BME on Anxiety Behaviour in Rotenone-Affected Mice

The elevated plus maze test was used to assess anxiety in rotenone-affected mice and BME-treated mice. Our data suggest that rotenone-affected mice tend to spend significantly less time and number of entries in open arms than in the control mice ($p < 0.05$) showing anxious behaviour, whereas BME pre-treated mice showed significantly ($p < 0.05$) more time spent and number of entries in the open arm. Furthermore, the BME post-treated mice also showed a significant elevation in the time spent and number of entries in open arm but it did not improve equally as seen in BME pre-treatment (Fig. 3D, E).

Effect of BME on the Expression of AMPAR Subunits GluR1 Transcript in the Hippocampus of Rotenone-Affected Mice

Quantitative real-time PCR data showed a significant rise in the expression of GluR1-AMPAR subunit mRNA in the hippocampus of rotenone-affected mice, as compared to the control mice ($p < 0.05$) whereas both pre-and post-treatment of rotenone-affected mice with BME led to a significant reversal of its expression compared to that in the rotenone-affected mice ($p < 0.05$) (Fig. 4A). The Western blot analysis demonstrated that treatment with BME significantly declined the elevated expression of the GluR1 subunit in rotenone-affected mice ($p < 0.05$) (Fig. 4B, C). Furthermore, immunofluorescence analysis of GluR1 transcript indicated a significant increase in immunoreactivity in the DG, CA1, and CA3 regions of the hippocampus of rotenone-affected mice compared to the control group mice. In the control group, most of the cells exhibited a consistent distribution and intensity of the GluR1 signal (Fig. 4D–I). In contrast, a significant reduction in immunoreactivity was found in the same areas of the hippocampus in rotenone-affected mice as a result of both pre- and post-BME treatment (Fig. 4D–I). However, the pre-BME treatment had a higher ameliorating potential than the post-BME treatment.

Effect of BME on the Expression of AMPAR Subunits GluR2 Transcript in the Hippocampus of Rotenone-Affected Mice

The quantitative RT-PCR investigation of the GluR2 subunit of the AMPA receptor mRNA expression in the hippocampus regions of rotenone-affected mice showed a significantly reduced expression of GluR2-AMPAR subunit mRNA compared to the control mice ($p < 0.05$). Unlike the rotenone-affected mice, the mice treated with BME, both before and after, exhibited a significant elevation in its expression ($p < 0.05$) (Fig. 5A). However, there is a significant distinction between the two BME doses, indicating that administering BME before rotenone treat had a more positive impact compared to administering it after rotenone effects. The Western blot findings revealed a significant decline in the expression of the GluR2 subunit compared to the control mice ($p < 0.05$). Compared to rotenone-affected mice, both the pre- and post-treated BME groups showed a significant increase in the expression of GluR2 (Fig. 5B, C). However, the pre-treatment resulted in a greater elevation in expression compared to the post-treatment of BME. Furthermore, like immunoblotting expression trends, the immunofluorescence examination of GluR2 revealed significantly reduced immunoreactivity in the DG, CA1, and CA3 regions of the hippocampus of rotenone-affected mice compared to the control group of mice. Conversely, in both pre- and post-BME-treated mice, significantly increased immunoreactivity was observed in the hippocampus regions of rotenone-affected mice (Fig. 5D–I). However, in this scenario, the pre-BME treatment exerted a significantly greater ameliorating potential than in the post-BME treatment mice group.

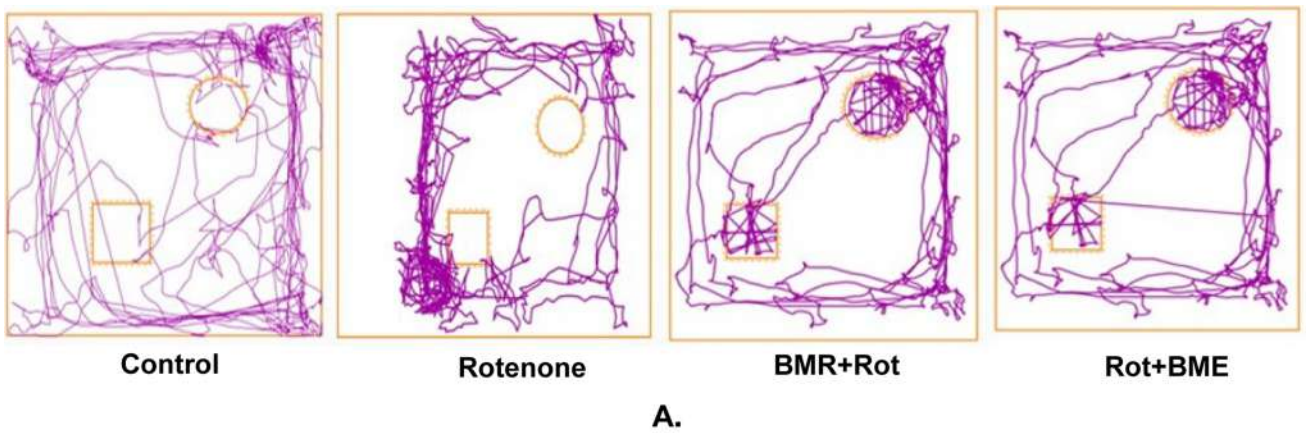
Control
Rotenone
BMR+Rot
Rot+BME

A.

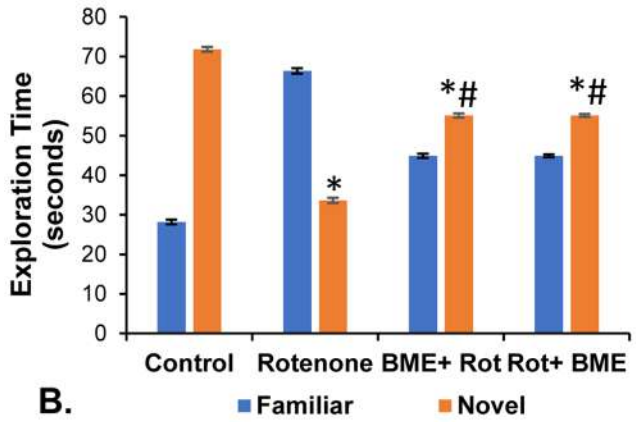
Exploration Time (seconds)
80
70
60
50
40
30
20
10
0
*
*#
*#
Control
Rotenone
BME+ Rot
Rot+ BME
Familiar
Novel

B.

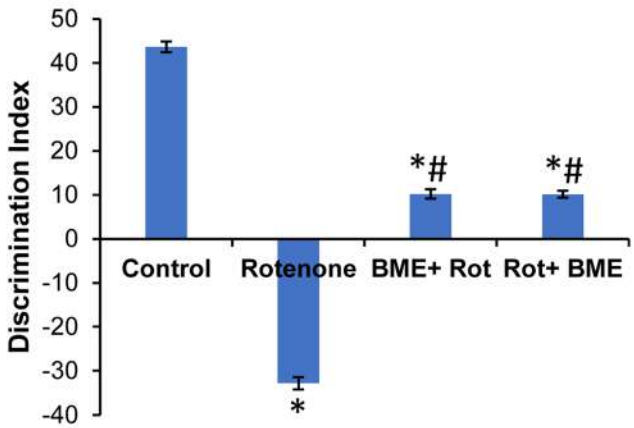
Discrimination Index
50
40
30
20
10
0
-10
-20
-30
-40
*
*#
*#
Control
Rotenone
BME+ Rot
Rot+ BME

C.

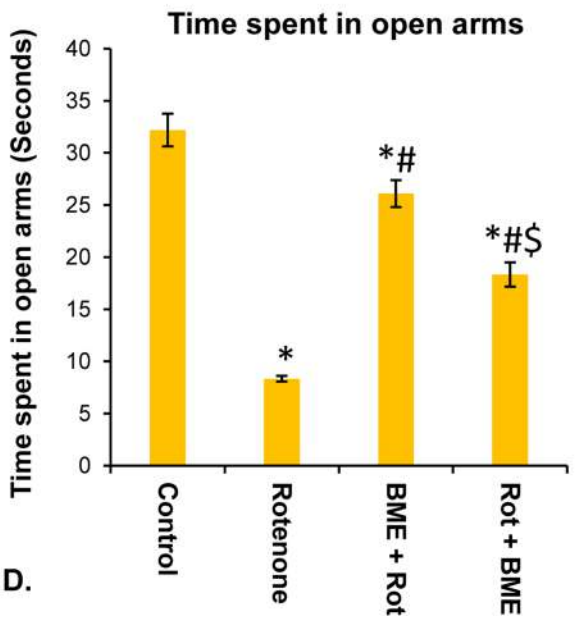
Time spent in open arms
Time spent in open arms (Seconds)
40
35
30
25
20
15
10
5
0
*
*#
*#$
Control
Rotenone
BME + Rot
Rot + BME

D.

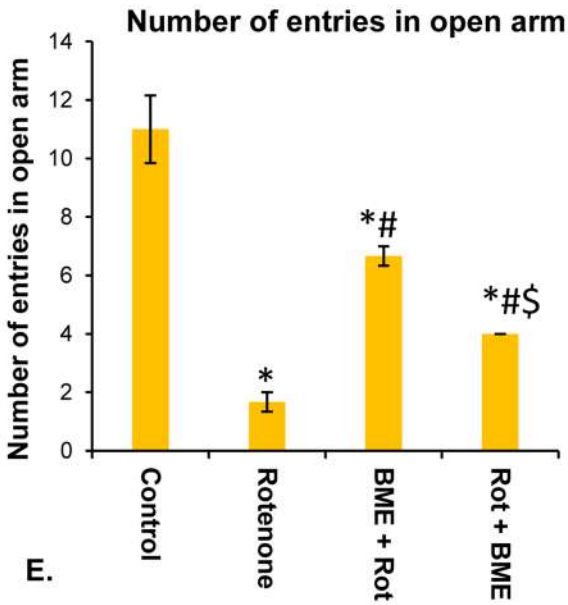
Number of entries in open arm
Number of entries in open arm
14
12
10
8
6
4
2
0
*
*#
*#$
Control
Rotenone
BME + Rot
Rot + BME

E.

◂**Fig. 3** Effect of BME (CDRI-08) on recognition memory and anxiety-like behaviour of vehicle-treated control, rotenone-affected mice (PD), pre-BME-treated PD mice, and post-BME-treated PD mice. Track plot of mice in novel object [round shape] and familiar object [square shape] in recognition test box (**A**); time spent (Sec) by mice with novel and familiar objects (**B**); discrimination index (**C**); time spent (Sec) in open arm of EPM (**D**); no. of entries in open arm of EPM (**E**); data represent mean ± SEM; *, significant difference ($p < 0.05$) between control and other groups; #, significant difference ($p < 0.05$) between rotenone and BME groups; $, significant difference ($p < 0.05$) between BME + Rot and Rot + BME groups

Effect of BME on the Expression of Trafficking Proteins in the Hippocampus of Rotenone-Affected Mice

The Western blot analysis data on the expression of AMPAR trafficking proteins revealed that the expression of TARPγ-2, PICK1, and PSD-95 was significantly higher in the rotenone-affected mice than in the control group ($p < 0.05$). Furthermore, TARPγ-2, PICK1, and PSD-95 expression were significantly lower in the pre- and post-treated BME groups than in the rotenone-affected mice. On the other hand, expression was lower following pre-BME treatment than following post-BME treatment (Fig. 6A–D).

Effect of BME on the Expression of CREB, pCREB, and BDNF in the Hippocampus of Rotenone-Affected Mice

The Western blot analysis data on the above proteins showed a significant decrease in the CREB, pCREB, and BDNF protein levels in the hippocampus of the rotenone-affected mice compared to that in the control group ($p < 0.05$). However, the pre-treatment with BME upregulated the CREB, pCREB, and BDNF protein expression ($p < 0.05$), and the expression of CREB and pCREB was found comparable to the control group. The upregulation of the CREB and BDNF expression in post-BME-treated PD mice was significantly higher. However, the amelioration of pCREB in post-treatment mice group was lesser compared to the pre-treatment condition (Fig. 7A–C).

Effects of CDRI-08 on the Neuronal Density of Various Hippocampal Regions in Rotenone-Affected Mice

The neuronal cell density was assessed by the cresyl violet staining (Nissl's staining) of the hippocampus in the brain sections. The results from Nissl's staining indicate a reduction in the density of viable neuronal cells in the DG, CA3, and CA1 area of the hippocampus in the rotenone-affected mice as compared to the control mice (Fig. 8A). Pre-treatment with BME demonstrated an increase in neuronal density in the post-rotenone-affected mice with BME and exhibited a substantial restoration in density. The pictorial images illustrate that BME therapy effectively reinstates the altered neuronal cell density to levels comparable to those in normal control animals. Nevertheless, the pre-BME treatment appears to have a more pronounced effect in sustaining neuronal cell density when compared to the post-BME treatment mice group.

Effect of BME on the Expression of Cleaved Caspase-3 in the Hippocampus of Rotenone-Affected Mice

The Western blot analysis showed a significant increase in the cleaved Caspase-3 protein levels in the hippocampus of mice with rotenone-affected mice compared to the control group ($p < 0.05$). However, pre-treatment with BME downregulated the cleaved Caspase-3 protein levels ($p < 0.05$), and the expression of cleaved Caspase-3 was found comparable to the control group. The significant downregulation of cleaved Caspase-3 expression was found in post-BME-treated rotenone-affected mice. However, pre-treatment with BME showed more significant improvement than in the post-BME treatment mice group (Fig. 8B and C).

Discussion

This study specifically investigates the cognitive impairments caused by rotenone-induced PD like conditiond through changes in the expression of proteins related to synaptic plasticity. It also explores the potential of *Bacopa monnieri* extract (CDRI-08) in protecting the brain by restoring rotenone-induced alterations in these proteins in mouse model. Rotenone is recognized for its ability to develop an effective model of Parkinson's disease (PD) by inhibiting complex-I of mitochondria, and inducing neurodegeneration [49, 50]. Thus, we developed a PD mouse model by administering a selected dose of rotenone subcutaneously and validated it with motor behaviour tests. Parkinson's disease (PD) is characterized by motor impairment, including muscle weakness, sluggish or impaired movement, coordination defects, and poor body balance [51]. Our result indicates that rotenone-affected mice showed reduced grip strength and motor coordination as evidenced by the observed symptoms (Fig. 1A and B). However, the administration of BME (CDRI-08) considerably improves these impairments.

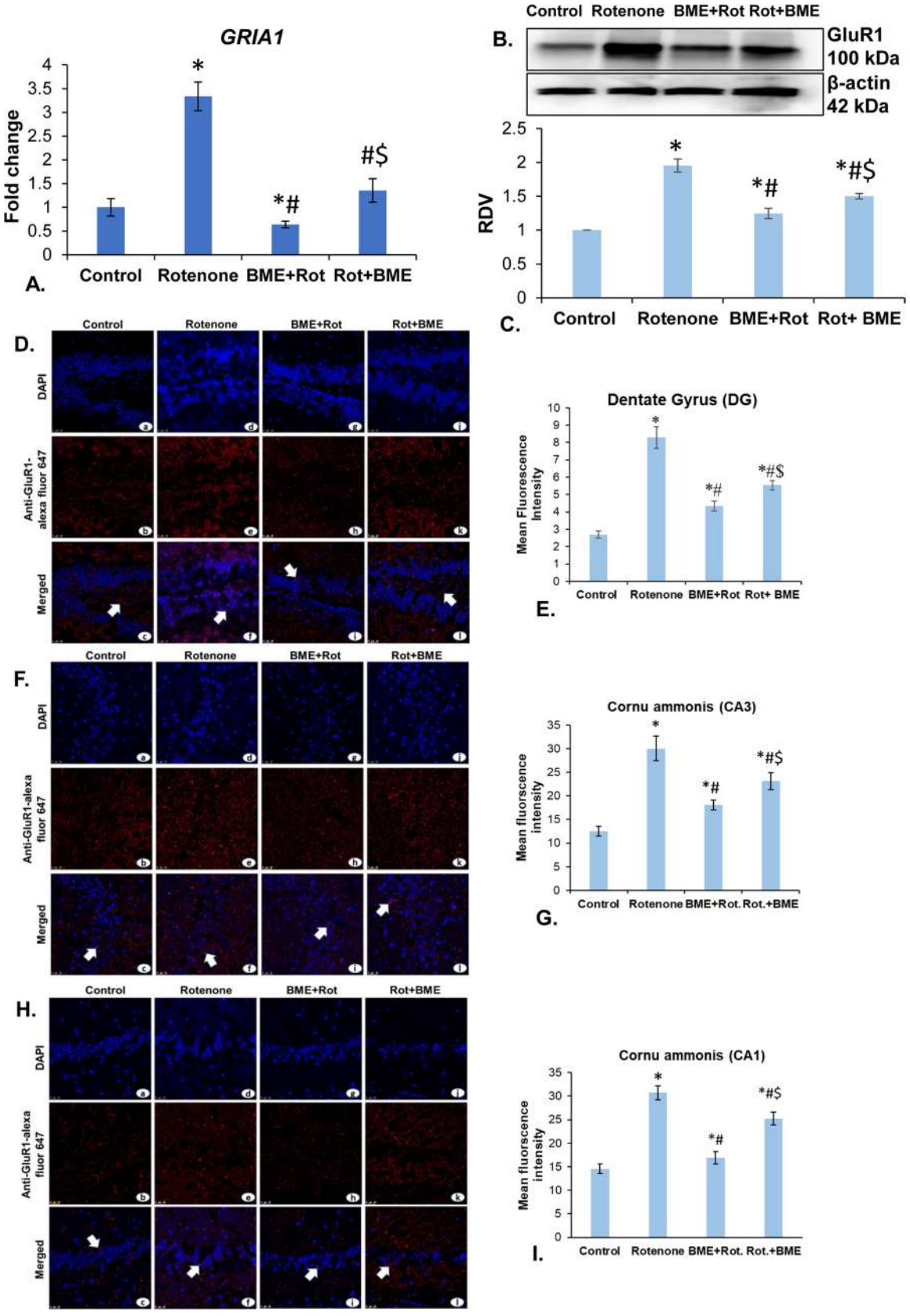
GRIA1
Fold change
Control
Rotenone
BME+Rot
Rot+BME
A.
B.
GluR1
100 kDa
β-actin
42 kDa
RDV
C.
D.
DAPI
Anti-GluR1-alexa fluor 647
Merged
E.
Dentate Gyrus (DG)
Mean Fluorescence Intensity
F.
G.
Cornu ammonis (CA3)
Mean fluorscence intensity
H.
I.
Cornu ammonis (CA1)

◂**Fig. 4** Effects of BME (CDRI-08) on the expression of GluR1 AMPA receptor subunit in the hippocampus of vehicle-treated control, rotenone-affected mice (PD), pre-BME-treated PD mice (BME + Rot), and post-BME-treated PD mice (Rot + BME). Histograms represent fold change of GluR1 (*GRIA-1*) mRNA level (**A**); Western blot of GluR1 and β-actin (**B**); histogram representing RDV of GluR1 (IDV of GluR1/IDV of β-actin) (**C**); photomicrographs show immunofluorescence showing TRITC-labelled signals of GluR1 in DG (**D**), CA3 (**F**), and CA1 (**H**) regions of hippocampus; histograms represent mean fluorescence intensity of DG (**E**), CA3 (**G**), and CA1 (**I**) regions of hippocampus. Data represent mean ± SEM; *, a significant difference ($p < 0.05$) between control and other groups; #, a significant difference ($p < 0.05$) between rotenone (PD) and BME groups; $, significant difference ($p < 0.05$) between BME + Rot and Rot + BME groups

Nevertheless, pre-treatment of BME exhibits a more noticeable impact, indicating that the preventive influence of BME on motor symptoms holds greater potential than its therapeutic effect.

The presence of Lewy bodies serves as evidence for the occurrence of Parkinson's disease. Lewy bodies are formed by the accumulation of mis-folded α-Synuclein protein and are recognized as a characteristic feature of Parkinson's disease [2]. The accumulation of pathogenic α-Synuclein protein leads to a decrease in synaptic plasticity–related proteins, neuronal excitability, and connectivity that ultimately leads to neuronal death. Our work revealed that treatment with BME (CDRI-08) successfully decreased the heightened expression of α-Synuclein monomer in the hippocampal subregions (DG, CA3, and CA1) restoring it to its normal levels (Fig. 2). The upregulation of α-Synuclein monomer may lead to the formation of α-Syn oligomers by aberrant aggregation, which can ultimately serve as precursors for Lewy bodies [52]. The abnormal accumulation of α-Syn protein initiates neuronal cell death by impairing the activities of lysosomes and mitochondria and disrupting calcium balance. Furthermore, it has been revealed that the accumulation of α-Syn in dementia, multiple system atrophy, and REM sleep behaviour disorder is responsible for initiating the process of neurodegeneration [53]. This process has also been linked to a decline in memory and cognitive function of the brain [54].

In this context, our NOR test data revealed that the rotenone-affected mice exhibited a significant reduction in the amount of time they spent for exploring novel things and instead focused their attention on objects they were already familiar with (Fig. 3B). In addition, they displayed an inability to distinguish between the new objects and that one which they had previously encountered (Fig. 3C). Both doses of BME (CDRI-08) exhibit equivalent efficacy in enhancing the condition. In addition to NOR, we examined the anxiety level in rotenone-affected mice by elevated plus maze test to know the rotenone's effects on exploration, curiosity, and overall mice activity. Our data revealed that the rotenone-affected mice spent less time in the open arm than in the control mice exhibiting more anxious behaviour. Further, the BME treatment improved the above-mentioned alterations towards that in the normal control mice. This can be co-related with the NOR test findings as reduced anxiety could lead to more exploration and interest in novel objects (Fig. 3D, E).

AMPA and NMDA receptors are the major players in the mechanism of synaptic plasticity [13]. Changes in the properties and quantity of AMPA receptor subunits have a notable impact on modifying synaptic plasticity, such as long-term potentiation (LTP), long-term depression (LTD), and glutamate and Ca^{2+} homeostasis. The results obtained from our qRT-PCR, Western blot, and immunofluorescence (IFC) experiments indicate that the expression levels of GluR1 and GluR2 subunits (Figs. 4 and 5) suggest that rotenone-induced PD condition leads to a significant increase in GluR1 subunit expression and a notable decrease in GluR2 subunit expression in the hippocampus and its subregions including the DG, CA3, and CA1. The finding indicates that the GluR1 subunit which is responsible for facilitating the influx of Ca^{2+} ions is more prevalent in the postsynaptic membrane in rotenone-induced Parkinson's disease condition [55]. Consequently, these neurons are more prone to get more excitation as a result of an increased influx of Ca^{2+} ions leading to excitotoxicity. Conversely, the GluR2 subunit containing AMPA receptor, which is impermeable to Ca^{2+} ions, is found at lower levels in the postsynaptic membrane in rotenone-affected mice. Activation of the NMDA receptor due to this condition can potentially amplify the postsynaptic current, resulting in neuronal toxicity and subsequent cell death. These alterations may be linked to decrease in memory and thus the cognitive function as observed in rotenone-affected PD mice in our study. However, the BME (CDRI-08) effectively reversed the changes in the expression of these two subunits. Nevertheless, the pre-treatment of BME has a more significant impact compared to the post-treatment, condition indicating its possible neuroprotective effect through enhancing brain connectivity, communication, and signal transmission. The restoration process may be attributed to an enhancement in the performance of mice as revealed from our NOR test data on recognition memory. The increase in GluR1 containing Ca^{2+} permeable AMPAR causes the membrane to become more depolarized leading to activation of large number of NMDA receptors on the postsynaptic membrane. Furthermore, this condition may lead to a rapid synaptic response [56, 57] and lead to the development of excitotoxicity [58].

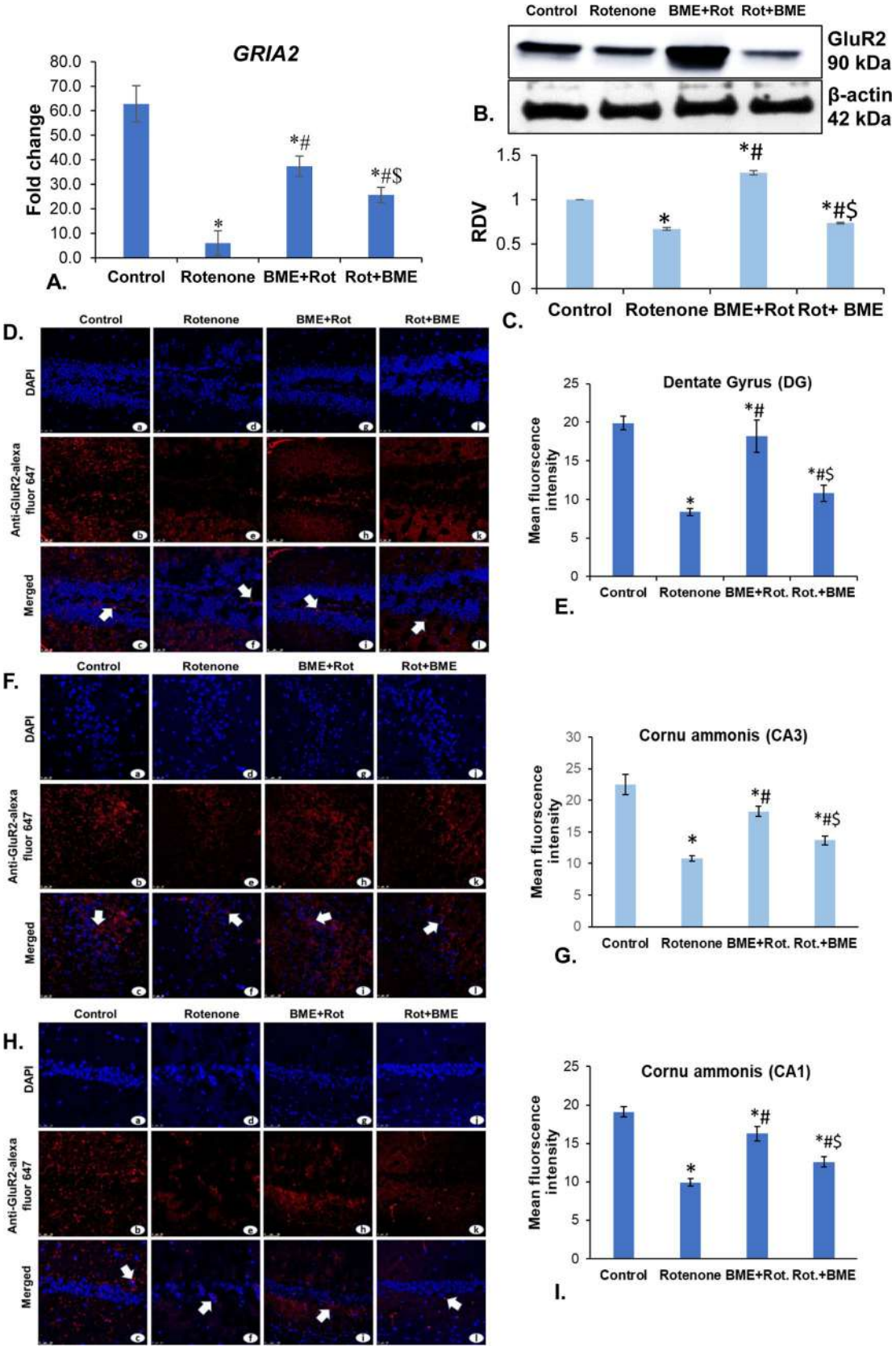
GRIA2
Fold change
80.0
70.0
60.0
50.0
40.0
30.0
20.0
10.0
0.0
*
*#
*#$
A.
Control
Rotenone
BME+Rot
Rot+BME
Control Rotenone BME+Rot Rot+BME
GluR2
90 kDa
β-actin
42 kDa
B.
RDV
1.5
1
0.5
0
*
*#
*#$
C.
Control Rotenone BME+Rot Rot+ BME
D.
Control
Rotenone
BME+Rot
Rot+BME
DAPI
Anti-GluR2-alexa fluor 647
Merged
Dentate Gyrus (DG)
Mean fluorscence intensity
25
20
15
10
5
0
E.
Control Rotenone BME+Rot. Rot.+BME
F.
Cornu ammonis (CA3)
30
25
20
15
10
5
0
G.
H.
Cornu ammonis (CA1)
I.

◂**Fig. 5** Effect of BME (CDRI-08) on the expression of GluR2 in the hippocampus of vehicle-treated control, rotenone-affected mice (PD), pre-BME-treated PD mice (BME + Rot), and post-BME-treated PD mice (Rot + BME). Histograms represent fold change in the level of GluR2 (*GRIA-2*) mRNA expression (**A**); Western blot of GluR2 and β-actin (**B**); histograms represent RDV of GluR2 (IDV of GluR2/IDV of β-actin) (**C**); photomicrographs show immunofluorescence illustrating TRITC-labelled signals of GluR1 in DG (**D**), CA3 (**F**), and CA1 (**H**) region of hippocampus; histogram representing mean fluorescence intensity of DG (**E**), CA3 (**G**), and CA1 (**I**) region of hippocampus. Data represent mean ± SEM; *, a significant difference ($p < 0.05$) between control and other groups; #, a significant difference ($p < 0.05$) between rotenone and BME groups; $, significant difference ($p < 0.05$) between BME + Rot and Rot + BME groups

The AMPAR trafficking proteins like TARP γ-2, PICK1, and PSD-95 play crucial role in the control of synaptic strength, receptor trafficking, and signalling complex assembly at excitatory synapses. Interaction of these proteins with AMPA receptors controls synaptic plasticity, a crucial process for learning and memory. Disturbance in this process could be a factor in memory-related illnesses or cognitive deficits. The expression of PICK1 was significantly increased in rotenone-affected mice (Fig. 6). Elevated levels of PICK1 in neurons result in reduced level of GluR2 on the postsynaptic density as PICK1 facilitates the internalization of AMPA receptors [59]. Thus, in the rotenone-affected PD mice, the increased expression of PICK1 might be correlated with an increased internalization of AMPA receptors containing GluR2 subunit on the postsynaptic membrane. In addition, there is a higher abundance of AMPA receptors that contain GluR1 subunit on the postsynaptic membrane. PSD-95 and TARPγ-2 are two crucial proteins that play role in stabilizing the AMPA receptor on the postsynaptic cell membrane [60, 61]. A significant increase in the expression of PSD-95 was observed in rotenone-affected mice compared to control mice. Moreover, there was a substantial increase in the expression of TARPγ-2 in the rotenone-induced PD mice. Nevertheless, the rotenone-affected mice exhibited a restoration of normal levels of PSD-95 and TARPγ-2 when they were administered BME in both pre- and post-treatment (Fig. 6). This finding suggests that the application of pre-BME treatment had a much more pronounced impact on all three trafficking proteins in comparison to rotenone-treated mice administered with the BME treatment. The results indicate the interaction between PSD-95 and TARPγ-2, as well as other members of the TARP family establish their connection to AMPA receptors on the postsynaptic membrane. In addition, they interact with the PDZ domains of PSD-95 via their C-terminal domains. The connection between PSD-95 and TARPγ-2 is believed to strengthen

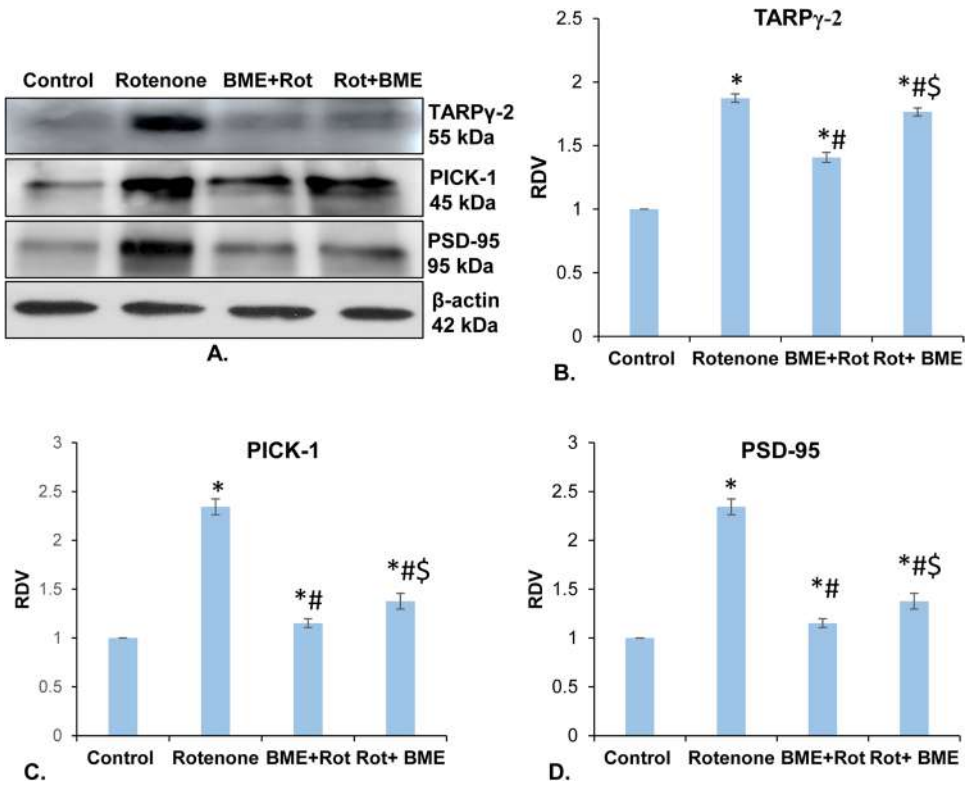

Fig. 6 Effects of BME (CDRI-08) on the expression of trafficking proteins of AMPAR in the hippocampus of vehicle-treated control, rotenone-affected mice (PD), pre-BME-treated PD mice (BME + Rot), and post-BME-treated PD mice (Rot + BME). Western blot of TARPγ-2, PICK-1, PSD-95, and β-actin (**A**). Histograms represent RDV of TARPγ-2, PICK-1, and PSD-95 (IDV of TARPγ-2, PICK-1, PSD-95/IDV of β-actin) (**B**, **C**, and **D**). Data represent mean ± SEM; *, a significant difference ($p < 0.05$) between control and other groups; #, a significant difference ($p < 0.05$) between rotenone and BME groups; $, significant difference ($p < 0.05$) between BME + Rot and Rot + BME groups

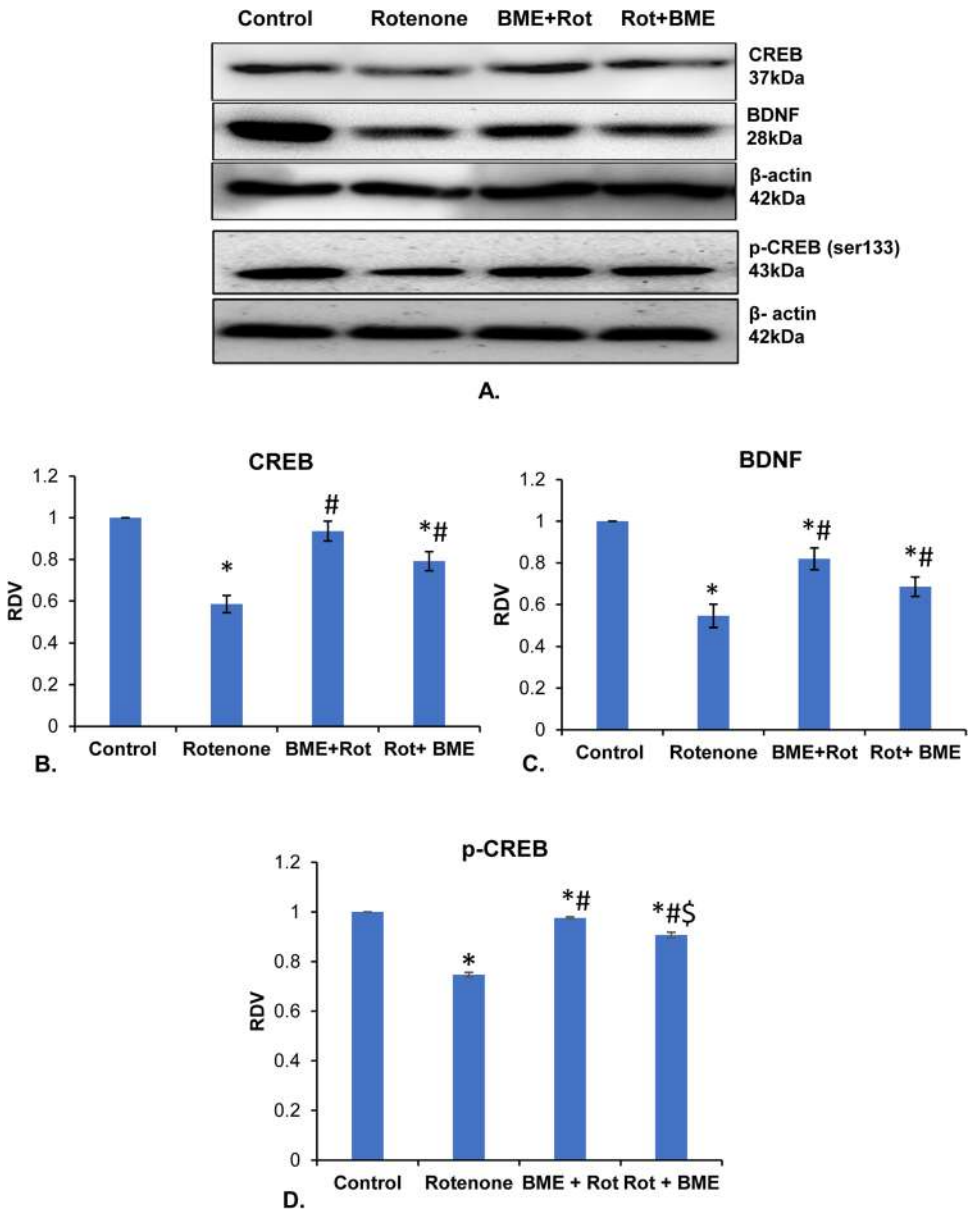

Fig. 7 Effects of BME (CDRI-08) on the expression of CREB, BDNF, and pCREB, BDNF, in the hippocampus of vehicle-treated control, rotenone-affected mice (PD), pre-BME-treated PD mice (BME + Rot), and post-BME-treated PD mice (Rot + BME). Western blot of CREB, BDNF, and pCREB, and β-actin (**A**). Histograms represent RDV of CREB, BDNF, and pCREB (IDV of CREB, BDNF, and pCREB/IDV of β-actin) (**B**–**D**). Data represent mean ± SEM; *, a significant difference ($p < 0.05$) between control and other groups; #, a significant difference ($p < 0.05$) between rotenone and BME groups; $, significant difference ($p < 0.05$) between BME + Rot and Rot + BME groups

the stability of the receptors by linking them to PSD. The connection between TARPs and PSD-95 is crucial for the localization of AMPA receptors synaptic density [62, 63]. Consequently, the increased level of PSD-95 and TARPγ-2 in rotenone-induced PD-like condition suggest that the large number of AMPA receptor is expressed on the postsynaptic membrane in PD-like condition which might lead to over activation of NMDA receptor that eventually may induce continual influx of Ca^{2+} into the postsynaptic neurons.

Recent investigations have indicated that the stimulation of extra-synaptic NMDA receptors containing GluN2B subunits leads to persistent dephosphorylation of CREB, which is referred to as CREB shut-off [63]. As a result, CREB becomes transcriptionally inactive due to its fast dephosphorylation at serine-133 [64]. Our result indicates that an increase in Ca^{2+}-permeable AMPA receptors can initiate NMDA downstream signalling that may potentially lead to the activation of the CREB shut-off pathway in Parkinson's disease–like condition. Consequently, this

impedes the activation of genes associated with plasticity such as BDNF. This may result in impaired synaptic function, synapse loss, and eventually a condition of neuronal death [64, 65]. Our data on the expression of CREB, pCREB, and BDNF provide evidence for this notion, as we observe a significant decrease in their expression in rotenone-induced PD mice (Fig. 7A–D). This suggests that there is a disruption in synaptic plasticity, which in turn leads to cognitive impairment. In addition, the BME (CDRI-08) enhances the levels of CREB, pCREB, and BDNF expression in both pre- and post-BME treatment. However, the pre-BME treatment showed a better effect than post-BME treatment in the upregulation of the pCREB. Our data indicates that BME (CDRI-08) possesses both memory-enhancing and neurotherapeutic effects on cognitive impairment.

To examine whether the rotenone treatment caused excitotoxic condition leading to neuronal death, we systematically assessed neurodegeneration in mice exposed to rotenone. Further, we also studied whether rotenone-induced neurodegeneration was due to amplified apoptotic death and thereby memory impairment. Our Nissl staining results showed a significant reduction in neuronal cell count in rotenone-affected mice compared to that in the control group. Notably, the BME pre-treatment conferred neuronal protection as evident in a neuronal density closely resembling that of the control group. This underscores the neuroprotective effects of BME. Conversely, BME post-treatment also demonstrates a capacity to enhance cell density, albeit not to the same extent as with BME pre-treatment. The observed improvement in cell density, however, remains notable and supports the potential therapeutic impact of BME, albeit with a clear distinction between pre-treatment and post-treatment applications.

In order to demonstrate whether the decline in the neuronal cell density in the hippocampal regions is due to apoptosis, we examined the expression of the active form of the Caspase-3 enzyme known as cleaved Caspase-3 as this is an important marker of the apoptotic neuronal death leading to neurodegeneration. Our data clearly showed elevated expression of the cleaved Caspase-3 in rotenone-affected mice compared to that in the control mice. This evidently confirmed that the rotenone-induced decline in the neuronal cell density was due to apoptotic cell death in the hippocampus. Our finding, on the other hand, exhibited the anti-apoptotic effect of BME as demonstrated by significantly decreased expression of cleaved Caspase-3 in the hippocampus of rotenone-affected PD mice with BME pre-treatment. However, the anti-apoptotic effects of BME were significantly more pronounced in pre-BME-treated mice compared to the post-BME treatment.

Altogether, our results show that BME has a nootropic effect that enhances recognition memory by lowering excitotoxicity by the operation of CREB shut-off pathway in synapses and it prevents apoptotic neurodegeneration. Consequently, *Bacopa monnieri* extract offers a promising neuroprotective and therapeutic for the PD-induced neurodegeneration led cognitive impairment.

Conclusion

The findings of our study provide an insight into a molecular cascade that links the impairment in motor behaviour and recognition memory caused by rotenone-induced PD like conditions with altered expression of the synaptic plasticity–related protein AMPA receptor (GluR1 and GluR2 subunits), its trafficking, and regulatory proteins that lead to excitotoxicity by BDNF downregulation and apoptotic neurodegeneration. Furthermore, both pre- and post-treatment with *Bacopa monnieri* extract (CDRI-08) has the ability to significantly recover the PD-associated alterations by differentially altering the expression of AMPA receptor, its trafficking proteins (TARPγ-2, PSD-95, and PICK1), and CREB shut-off pathway related proteins. This evidently indicates the potential therapeutic and nootropic effects of BME in rotenone-induced PD mimicking conditions in mice.

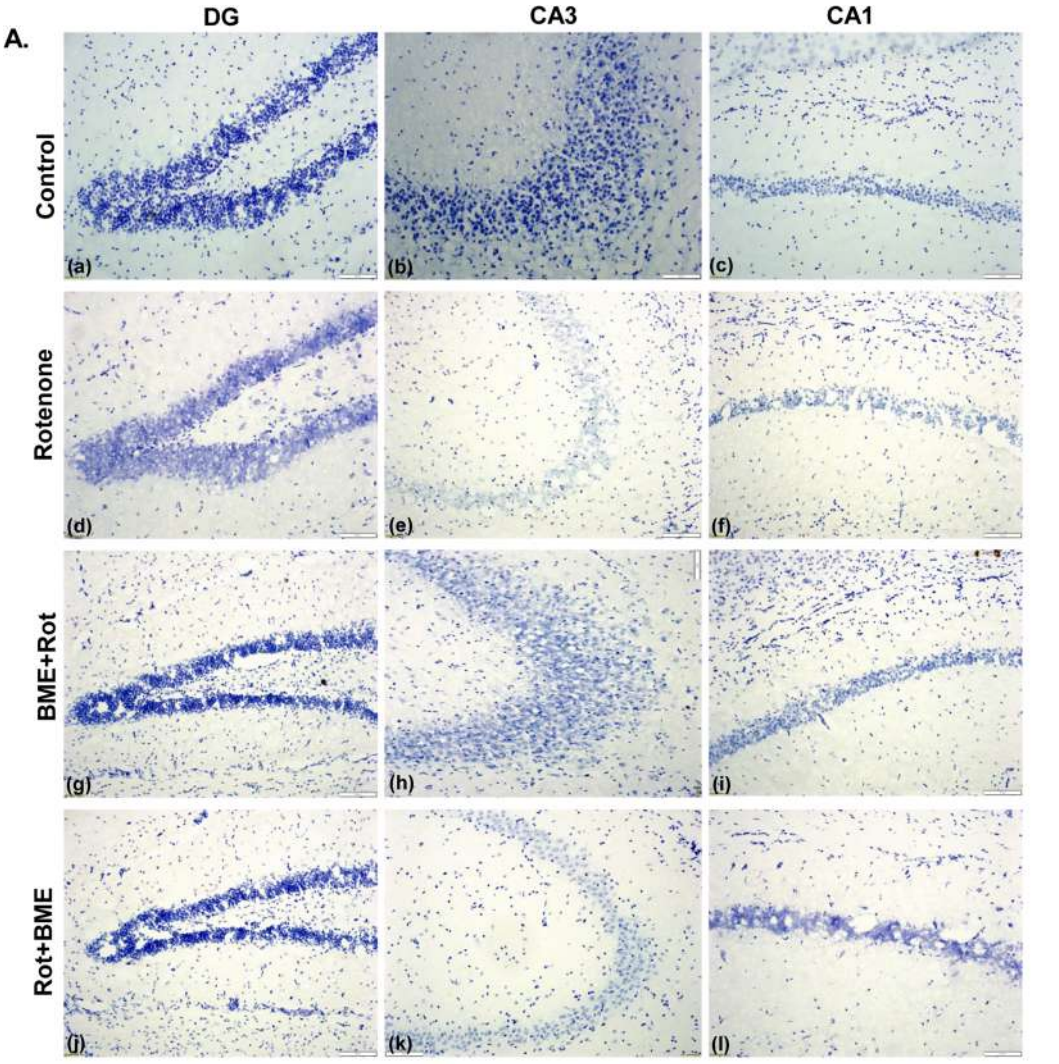
A.
DG
CA3
CA1
Control
Rotenone
BME+Rot
Rot+BME
(a)
(b)
(c)
(d)
(e)
(f)
(g)
(h)
(i)
(j)
(k)
(l)

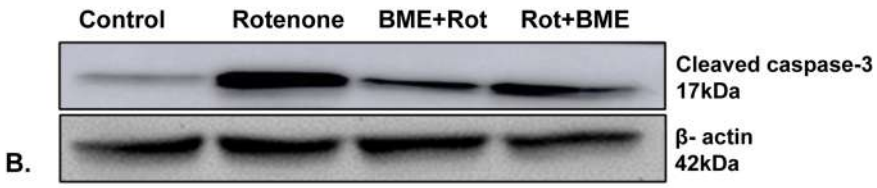
Control
Rotenone
BME+Rot
Rot+BME
Cleaved caspase-3
17kDa
β- actin
42kDa
B.

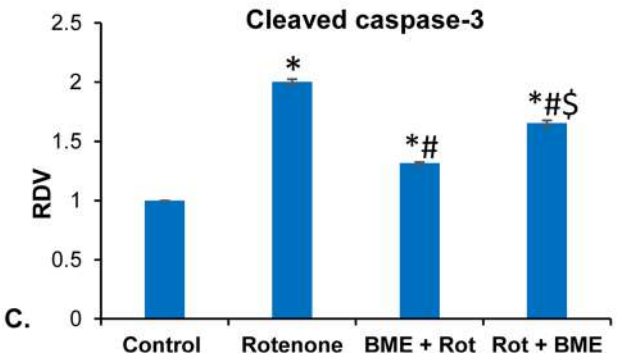
Cleaved caspase-3
RDV
2.5
2
1.5
1
0.5
0
*
*#
*#$
C.
Control
Rotenone
BME + Rot
Rot + BME

◂**Fig. 8** Effects of BME (CDRI-08) on neuronal cell density in hippocampal subregions (DG, CA3, and CA1) and on the expression of cleaved Caspase-3 in the hippocampus of vehicle-treated control, rotenone-affected mice (PD), pre-BME-treated PD mice (BME + Rot), and post-BME-treated PD mice (Rot + BME) (**A**). Western blot of cleaved Caspase-3 and β-actin (**B**). Histograms represent RDV of cleaved Caspase-3 (IDV of cleaved Caspase-3/IDV of β-actin) (**C**). Data present mean ± SEM; *, a significant difference ($p < 0.05$) between control and other groups; #, a significant difference ($p < 0.05$) between rotenone and BME groups; $, significant difference ($p < 0.05$) between BME + Rot and Rot + BME groups

Acknowledgements The authors are grateful to CAS and DST-FIST Level II programs, Department of Zoology, Central Discovery Centre under the SATHI Programs in Banaras Hindu University (BHU) for the Laser Scanning Super-Resolution Microscope System (Model: SP8 STED) facility and Interdisciplinary School of Life Sciences (ISLS), Banaras Hindu University (BHU) for real-time PCR. The authors acknowledge Dr. Hemant K Singh, Former Deputy Director of CSIR-CDRI, Govt. of India for generously providing the well-characterized extract of *Bacopa monnieri* (CDRI-08). VG acknowledges the University Grants Commission, Govt. of India for CSIR-UGC JRF and SRF.

Author Contribution Vartika Gupta: planned and carried out experiments, captured images, processed data, carried out statistical analysis of the result, and prepared draft manuscript. S. Prasad: generated funds, developed concept and planned experiment, interpreted the results, and edited and finalized the manuscript.

Funding This work was supported by funds from the Indian Council of Medical Research (ICMR), Govt. of India, Institute of Eminence (IoE), BHU, and partial financial support from CSIR, BRNS, and UGC, Govt. of India.

Data Availability The datasets analyzed during the study are available from the corresponding author upon reasonable request.

Declarations

Ethics Approval The present study was performed according to the guidelines of the Committee for Control and Supervision of Experiments on Animals (CPCSEA), and the Institutional Animal Ethical Committee of Banaras Hindu University, Varanasi, approved all experimental procedures (Approval no.: BHU/DOZ/IAEC/2021–2022/007, Dated 15/02/2022).

Consent to Participate Not applicable.

Consent for Publication Not applicable.

Competing Interests The authors declare no competing interests.

References

1. Tysnes OB, Storstein A (2017) Epidemiology of Parkinson's disease. J Neural Transm (Vienna, Austria: 1996) 124(8):901–905. https://doi.org/10.1007/s00702-017-1686-y
2. Mehra S, Sahay S, Maji SK (2019) α-Synuclein misfolding and aggregation: implications in Parkinson's disease pathogenesis. Biochim Biophys Acta Protein Proteomics 1867(10):890–908. https://doi.org/10.1016/j.bbapap.2019.03.001
3. Balestrino R, Schapira AHV (2020) Parkinson disease. Eur J Neurology 27(1):27–42. https://doi.org/10.1111/ene.14108
4. Vidović M, Rikalovic MG (2022) Alpha-Synuclein aggregation pathway in Parkinson's disease: current status and novel therapeutic Approaches. Cells 11(11):1732. https://doi.org/10.3390/cells11111732
5. Aarsland D, Batzu L, Halliday GM, Geurtsen GJ, Ballard C, Ray Chaudhuri K, Weintraub D (2021) Parkinson disease-associated cognitive impairment. Nat Rev Dis Primers 7(1):47. https://doi.org/10.1038/s41572-021-00280-3
6. Aarsland D, Creese B, Politis M, Chaudhuri KR, Ffytche DH, Weintraub D, Ballard C (2017) Cognitive decline in Parkinson disease. Nat Rev Neurol 13(4):217–231. https://doi.org/10.1038/nrneurol.2017.27
7. Das T, Hwang JJ, Poston KL (2019) Episodic recognition memory and the hippocampus in Parkinson's disease: a review. Cortex: A Journal Devoted to the Study of the Nervous System and Behavior 113:191–209.https://doi.org/10.1016/j.cortex.2018.11.021
8. Gomperts SN (2016) Lewy body dementias: dementia with Lewy bodies and Parkinson disease dementia. Continuum (Minneapolis, Minn.) 22(2 Dementia):435–463. https://doi.org/10.1212/CON.0000000000000309
9. Sezgin M, Bilgic B, Tinaz S, Emre M (2019) Parkinson's disease dementia and Lewy body disease. Semin Neurol 39(2):274–282. https://doi.org/10.1055/s-0039-1678579
10. Lu B, Nagappan G, Lu Y (2014) BDNF and synaptic plasticity, cognitive function, and dysfunction. Handb Exp Pharmacol 220:223–250. https://doi.org/10.1007/978-3-642-45106-5_9
11. Magee JC, Grienberger C (2020) Synaptic plasticity forms and functions. Annu Rev Neurosci 43:95–117. https://doi.org/10.1146/annurev-neuro-090919-022842
12. Malenka RC, Bear MF (2004) LTP and LTD: an embarrassment of riches. Neuron 44(1):5–21. https://doi.org/10.1016/j.neuron.2004.09.012
13. Diering GH, Huganir RL (2018) The AMPA receptor code of synaptic plasticity. Neuron 100(2):314–329. https://doi.org/10.1016/j.neuron.2018.10.018
14. Effendy MA, Yunusa S, Mat NH, Has ATC, Müller CP, Hassan Z (2023) The role of AMPA and NMDA receptors in mitragynine effects on hippocampal synaptic plasticity. Behav Brain Res 438:114169. https://doi.org/10.1016/j.bbr.2022.114169
15. Di Maio V, Ventriglia F, Santillo S (2016) AMPA/NMDA cooperativity and integration during a single synaptic event. J Comput Neurosci 41(2):127–142. https://doi.org/10.1007/s10827-016-0609-5
16 Qu WR, Sun QH, Liu QQ, Jin HJ, Cui RJ, Yang W, Song B, Li BJ (2020) Role of CPEB3 protein in learning and memory: new insights from synaptic plasticity. Aging 12(14):15169–15182. https://doi.org/10.18632/aging.103404
17. Li YH, Zhang N, Wang YN, Shen Y, Wang Y (2016) Multiple faces of protein interacting with C kinase 1 (PICK1): structure, function, and diseases. Neurochem Int 98:115–121. https://doi.org/10.1016/j.neuint.2016.03.001
18. Jiao Y, Fan H, Wang K, Lu S (2019) Sevoflurane impairs short-term memory by affecting PSD-95 and AMPA receptor in the hippocampus of a mouse model. Behav Neurol 2019:1068260. https://doi.org/10.1155/2019/1068260
19. Jackson AC, Nicoll RA (2011) Stargazin (TARP gamma-2) is required for compartment-specific AMPA receptor trafficking and synaptic plasticity in cerebellar stellate cells. J Neurosci : Off J Soc Neurosci 31(11):3939–3952. https://doi.org/10.1523/JNEUROSCI.5134-10.2011
20. Hollmann M, Heinemann S (1994) Cloned glutamate receptors. Annu Rev Neurosci 17:31–108. https://doi.org/10.1146/annurev.ne.17.030194.000335

21. Passafaro M, Piëch V, Sheng M (2001) Subunit-specific temporal and spatial patterns of AMPA receptor exocytosis in hippocampal neurons. Nat Neurosci 4(9):917–926. https://doi.org/10.1038/nn0901-917
22. Dingledine R, Borges K, Bowie D, Traynelis SF (1999) The glutamate receptor ion channels. Pharmacol Rev 51(1):7–61
23 Leal G, Comprido D, Duarte CB (2014) BDNF-induced local protein synthesis and synaptic plasticity. Neuropharmacology 76 Pt C:639–656. https://doi.org/10.1016/j.neuropharm.2013.04.005
24. Takeda H, Kitaoka Y, Hayashi Y, Kumai T, Munemasa Y, Fujino H, Kobayashi S, Ueno S (2007) Calcium/calmodulin-dependent protein kinase II regulates the phosphorylation of CREB in NMDA-induced retinal neurotoxicity. Brain Res 1184:306–315. https://doi.org/10.1016/j.brainres.2007.09.055
25. Sumathy T, Govindasamy S, Balakrishna K, Veluchamy G (2002) Protective role of Bacopa monniera on morphine-induced brain mitochondrial enzyme activity in rats. Fitoterapia 73(5):381–385. https://doi.org/10.1016/s0367-326x(02)00114-4
26. Banerjee S, Anand U, Ghosh S, Ray D, Ray P, Nandy S, Deshmukh GD, Tripathi V et al (2021) Bacosides from Bacopa monnieri extract: an overview of the effects on neurological disorders. Phytother Res : PTR 35(10):5668–5679. https://doi.org/10.1002/ptr.7203
27. Pathak A, Kulshreshtha DK, Maurya R (2005) Chemical constituents of Bacopa procumbens. Nat Prod Res 19(2):131–136. https://doi.org/10.1080/14786410410001704732
28. Ohta T, Nakamura S, Nakashima S, Oda Y, Matsumoto T, Fukaya M, Yano M, Yoshikawa M et al (2016) Chemical structures of constituents from the whole plant of Bacopa monniera. J Nat Med 70(3):404–411. https://doi.org/10.1007/s11418-016-0986-0
29. Aguiar S, Borowski T (2013) Neuropharmacological review of the nootropic herb Bacopa monnieri. Rejuvenation Res 16(4):313–326. https://doi.org/10.1089/rej.2013.1431
30. Jeyasri R, Muthuramalingam P, Adarshan S, Shin H, Ramesh M (2022) Assessing the anti-inflammatory effects of Bacopa-derived bioactive compounds using network pharmacology and *in vitro* studies. ACS Omega 7(44):40344–40354. https://doi.org/10.1021/acsomega.2c05318
31 Srivastav S, Fatima M, Mondal AC (2017) Important medicinal herbs in Parkinson's disease pharmacotherapy. Biomed Pharmacother = Biomed Pharmacother 92:856–863. https://doi.org/10.1016/j.biopha.2017.05.137
32. Walker EA, Pellegrini MV (2023) Bacopa monnieri. StatPearls Publishing, In StatPearls
33. Rai R, Singh HK, Prasad S (2015) A special extract of Bacopa monnieri (CDRI-08) restores learning and memory by upregulating expression of the NMDA receptor subunit GluN2B in the brain of scopolamine-induced amnesic mice. Evid-Based Complement Alternat Med :eCAM 2015:254303. https://doi.org/10.1155/2015/254303
34. Pandey SP, Singh HK, Prasad S (2015) Alterations in hippocampal oxidative stress, expression of AMPA receptor GluR2 subunit and associated spatial memory loss by Bacopa monnieri extract (CDRI-08) in streptozotocin-induced diabetes mellitus type 2 mice. PLoS ONE 10(7):e0131862. https://doi.org/10.1371/journal.pone.0131862
35. Singh HK, Rastogi RP, Srimal RC, Dhawan BN (1988) Effect of bacosides A and B on avoidance responses in rats. Phytother Res 2(2):70–75
36. Dhawan BN, Singh HK (1996) Pharmacological studies on Bacopa monniera, an Ayurvedic nootropic agent. Eur Neuropsychopharmacol 6:144
37. Singh HK, Dhawan BN (1997) Neuropsychopharmacological effects of the ayurvedic nootroplc Bacopa monnleralinn.(Brahmi). Indian J Pharmacol 29(5):359–365
38. Jeyasri R, Muthuramalingam P, Suba V, Ramesh M, Chen JT (2020) *Bacopa monnieri* and their bioactive compounds inferred multi-target treatment strategy for neurological diseases: a cheminformatics and system pharmacology approach. Biomolecules 10(4):536. https://doi.org/10.3390/biom10040536
39. Alkadhi KA (2019) Cellular and molecular differences between area ca1 and the dentate gyrus of the hippocampus. Mol Neurobiol 56(9):6566–6580. https://doi.org/10.1007/s12035-019-1541-2
40. Singh B, Pandey S, Verma R, Ansari JA, Mahdi AA (2016) Comparative evaluation of extract of Bacopa monnieri and Mucuna pruriens as neuroprotectant in MPTP model of Parkinson's disease. Indian J Exp Biol 54(11):758–766
41. Shiotsuki H, Yoshimi K, Shimo Y, Funayama M, Takamatsu Y, Ikeda K, Takahashi R, Kitazawa S et al (2010) A rotarod test for evaluation of motor skill learning. J Neurosci Methods 189(2):180–185. https://doi.org/10.1016/j.jneumeth.2010.03.026
42. Kraeuter AK, Guest PC, Sarnyai Z (2019) The elevated plus maze test for measuring anxiety-like behavior in rodents. Techniques and Protocols, Pre-Clinical Models, pp 69–74
43. Barman B, Kushwaha A, Thakur MK (2021) Vitamin B_{12}-folic acid supplementation regulates neuronal immediate early gene expression and improves hippocampal dendritic arborization and memory in old male mice. Neurochem Int 150:105181. https://doi.org/10.1016/j.neuint.2021.105181
44. Bradford MM (1976) A rapid and sensitive method for the quantitation of microgram quantities of protein utilizing the principle of protein-dye binding. Anal Biochem 72:248–254. https://doi.org/10.1006/abio.1976.9999
45. Singh K, Gaur P, Prasad S (2007) Fragile x mental retardation (Fmr-1) gene expression is down regulated in brain of mice during aging. Mol Biol Rep 34(3):173–181. https://doi.org/10.1007/s11033-006-9032-8
46. Gaur P, Prasad S (2014) Alterations in the Sp1 binding and Fmr-1 gene expression in the cortex of the brain during maturation and aging of mouse. Mol Biol Rep 41(10):6855–6863. https://doi.org/10.1007/s11033-014-3571-1
47. Rao X, Huang X, Zhou Z, Lin X (2013) An improvement of the 2ˆ(-delta delta CT) method for quantitative real-time polymerase chain reaction data analysis. Biostat Bioinforma Biomath 3(3):71–85
48 Dalvi PS, Belsham DD (2021) Immunofluorescence of GFAP and TNF-α in the mouse hypothalamus. Bio Protoc 11(13):e4078. https://doi.org/10.21769/BioProtoc.4078
49. Thakur P, Nehru B (2014) Modulatory effects of sodium salicylate on the factors affecting protein aggregation during rotenone induced Parkinson's disease pathology. Neurochem Int 75:1–10. https://doi.org/10.1016/j.neuint.2014.05.002
50. Konnova EA, Swanberg M (2018) Animal models of Parkinson's disease. In: Stoker TB (ed) Parkinson's disease: pathogenesis and clinical aspects. Codon Publications
51. Simon DK, Tanner CM, Brundin P (2020) Parkinson disease epidemiology, pathology, genetics, and pathophysiology. Clin Geriatr Med 36(1):1–12. https://doi.org/10.1016/j.cger.2019.08.002
52. Siddique A, Khan HF, Ali S, Abdullah A, Munir H, Ariff M (2020) Estimation of alpha-Synuclein monomer and oligomer levels in the saliva of the children with autism spectrum disorder: a possibility for an early diagnosis. Cureus 12(8):e9936. https://doi.org/10.7759/cureus.9936
53. Calabresi P, Mechelli A, Natale G, Volpicelli-Daley L, Di Lazzaro G, Ghiglieri V (2023) Alpha-synuclein in Parkinson's disease and other synucleinopathies: from overt neurodegeneration back to

early synaptic dysfunction. Cell Death Dis 14(3):176. https://doi.org/10.1038/s41419-023-05672-9
54. Volpicelli-Daley LA, Luk KC, Patel TP, Tanik SA, Riddle DM, Stieber A, Meaney DF, Trojanowski JQ et al (2011) Exogenous α-Synuclein fibrils induce Lewy body pathology leading to synaptic dysfunction and neuron death. Neuron 72(1):57–71. https://doi.org/10.1016/j.neuron.2011.08.033)
55. Jourdi H, Kabbaj M (2013) Acute BDNF treatment upregulates GluR1-SAP97 and GluR2-GRIP1 interactions: implications for sustained AMPA receptor expression. PLoS ONE 8(2):e57124. https://doi.org/10.1371/journal.pone.0057124)
56. Burnashev N, Monyer H, Seeburg PH, Sakmann B (1992) Divalent ion permeability of AMPA receptor channels is dominated by the edited form of a single subunit. Neuron 8(1):189–198. https://doi.org/10.1016/0896-6273(92)90120-3
57. Deng YP, Xie JP, Wang HB, Lei WL, Chen Q, Reiner A (2007) Differential localization of the GluR1 and GluR2 subunits of the AMPA-type glutamate receptor among striatal neuron types in rats. J Chem Neuroanat 33(4):167–192. https://doi.org/10.1016/j.jchemneu.2007.02.008
58. Essin K, Nistri A, Magazanik L (2002) Evaluation of GluR2 subunit involvement in AMPA receptor function of neonatal rat hypoglossal motoneurons. Eur J Neurosci 15(12):1899–1906. https://doi.org/10.1046/j.1460-9568.2002.02045.x
59. Lau A, Tymianski M (2010) Glutamate receptors, neurotoxicity and neurodegeneration. PflugersArchiv : Eur J Physiol 460(2):525–542. https://doi.org/10.1007/s00424-010-0809-1
60. Perez JL, Khatri L, Chang C, Srivastava S, Osten P, Ziff EB (2001) PICK1 targets activated protein kinase Calpha to AMPA receptor clusters in spines of hippocampal neurons and reduces surface levels of the AMPA-type glutamate receptor subunit 2. J Neurosci : Off J Soc Neurosci 21(15):5417–5428. https://doi.org/10.1523/JNEUROSCI.21-15-05417.2001
61. Hastie P, Ulbrich MH, Wang HL, Arant RJ, Lau AG, Zhang Z, Isacoff EY, Chen L (2013) AMPA receptor/TARP stoichiometry visualized by single-molecule subunit counting. Proc Natl Acad Sci USA 110(13):5163–5168. https://doi.org/10.1073/pnas.1218765110
62. Tomita S, Stein V, Stocker TJ, Nicoll RA, Bredt DS (2005) Bidirectional synaptic plasticity regulated by phosphorylation of stargazin-like TARPs. Neuron 45(2):269–277. https://doi.org/10.1016/j.neuron.2005.01.0092000
63. Ravi AS, Zeng M, Chen X, Sandoval G, Diaz-Alonso J, Zhang M, Nicoll RA (2022) Long-term potentiation reconstituted with an artificial TARP/PSD-95 complex. Cell Rep 41(2):111483. https://doi.org/10.1016/j.celrep.2022.111483)
64. Grochowska KM, Bär J, Gomes GM, Kreutz MR, Karpova A (2021) Jacob, a synapto-nuclear protein messenger linking N-methyl-D-aspartate receptor activation to nuclear gene expression. Front Synaptic Neurosci 13:787494. https://doi.org/10.3389/fnsyn.2021.787494
65. Mohanan AG, Gunasekaran S, Jacob RS, Omkumar RV (2022) Role of Ca^{2+}/calmodulin-dependent protein kinase type ii in mediating function and dysfunction at glutamatergic synapses. Front Mol Neurosci 15:855752. https://doi.org/10.3389/fnmol.2022.855752